





Computational Notes on The Effect of (Li-Na-K) on Calcium Zinc Phosphate Oxide Glasses

Medhtat A. Ibrahim¹ , Hend A. Ezzat² , Fanli Meng³, Ibrahim S. Yahia^{4,5,6} ,
Heba Y. Zahran^{4,5,6}, Hanan Elhaes⁷ 

¹ Molecular Spectroscopy and Modeling Unit, Spectroscopy Department, National Research Centre, 33 El-Bohouth Str. 12622 Dokki, Giza, Egypt

² Nano Technology Unit, Solar and Space Research Department, National Research Institute of Astronomy and Geophysics (Nano NRIAG), 11731 Helwan, Cairo, Egypt

³ College of Information Science and Engineering, Northeastern University, Shenyang 110819, China

⁴ Research Center for Advanced Materials Science (RCAMS), King Khalid University, Abha 61413, P.O. Box 9004, Saudi Arabia

⁵ Advanced Functional Materials & Optoelectronic Laboratory (AFMOL), Department of Physics, Faculty of Science, King Khalid University, P.O. Box 9004, Abha, Saudi Arabia

⁶ Nanoscience Laboratory for Environmental and Bio-Medical Applications (NLEBA), Semiconductor Lab., Metallurgical Lab. 2 Physics Department, Faculty of Education, Ain Shams University, Roxy, 11757 Cairo, Egypt

⁷ Physics Department, Faculty of Women for Arts, Science, and Education, AinShams University, 11757, Cairo, Egypt

* Correspondence: medahmed6@yahoo.com;

Scopus Author ID 8641587100

Received: 22.04.2020; Revised: 25.05.2020; Accepted: 26.05.2020; Published: 1.06.2020

Abstract: A model molecule for P_4O_{10} -ZnO-CaO is constructed to build Calcium Zinc Phosphate Oxide glasses. Then the effect of alkalis Li; Na and K upon the model molecule is studied with *ab initio* Hartree-Fockat HF/3-21G** level of theory. The overall aim is to evaluate the electronic properties of both the model molecules and alkali substituted molecules. The calculated parameters, including highest occupied molecular orbital/lowest unoccupied molecular orbital (HOMO/LUMO) bandgap energies; Total dipole moment (TDM) and molecular electrostatic potentials (MESP) are calculated. It has also been observed that the calculated TDM of the glassy system P_4O_{10} -ZnO-CaO is increased while the HOMO/LUMO band gap is decreased as an indication for the reactivity of the studied model molecules. The active sites for the studied models are described by the calculated MESP, which is confirming the results of both TDM and HOMO/LUMO.

Keywords: Phosphate glass; Nano metal oxides; Hartree-Fock; Alkali elements.

© 2020 by the authors. This article is an open-access article distributed under the terms and conditions of the Creative Commons Attribution (CC BY) license (<https://creativecommons.org/licenses/by/4.0/>).

1. Introduction

Many forms of glasses depend on their structure on phosphate glasses continue to be a topic for a variety of technological applications [1-3]. The molecular structure of phosphate glass shows different properties, which in turn dedicated to many different applications that are related to their molecular-level structures [4-6]. The addition of ZnO on phosphate glass affected the properties of phosphate glass [7-8]. Several studies were constructed on Calcium Zinc phosphate oxide glasses such as doping with Mg and Li [9-10]. Molecular modeling could be used alone and/or with the help of experimental molecular spectroscopic technique as a descriptive tool for the molecular structures of many systems and structures in different areas of science. Such computational techniques are now widely used to mimic the molecular behavior in chemistry, drug design, computational biology, and material science [11-16]. The

range of molecular systems is ranging from small chemical systems to large biological molecules and material assemblies. It was previously utilized to study P_4O_{10} -ZnO-CaO- Na_2O glasses doped with copper oxide [17]. The temperature-dependent constraint model of alkali phosphate glasses was established for considering the structural and topological role of the modifying ion sub-network constituted by alkali ions and their non-bonding oxygen coordination spheres [18]. Molecular dynamics (MD) simulations have given new insight into the structural motifs which affect the dissolution, which is not accessible to experimental methods [19]. It is an excellent tool to describe atomic-level structural information for phosphate-based bioactive glasses [20]. MS simulations could also give information about the effect of alkali upon phosphate-based glasses [21-22]. Based on these considerations, it is clear that different classes of computational modeling gave information about the systems, whereas the experimental approach is limited or even unavailable [23- 32]. Of course, glass systems are among these systems [33-34].

In this work, molecular modeling at HF/3-21G** is utilized to study the effect of Li-Na-K on Calcium Zinc Phosphate Oxide glasses.

2. Materials and Methods

All the studied structures are subjected to energy optimization, then some physical parameters are calculated. Total dipole moment and HOMO/LUMO bandgap energies and molecular electrostatic potential were calculated at a higher level of theory at HF/3-21G** using GAUSSIAN 09 software [35], which is implemented at Spectroscopy Department, National Research Centre, Egypt.

3. Results and Discussion

Before describing the results, it is important to describe how the model molecule is built. A model molecule of phosphate glass P_4O_{10} is built as indicated in figure 1, then ZnO, CaO in the nanoscale are added as indicated in figure 2. The metal oxides are added in the two of the three corners while in the last corner, as shown in figure 3, Li, Na, K are added respectively; accordingly, Li, Na, K are added separately to form three models. Table 1 presented the calculated HF/3-21G** TDM and HOMO/LUMO band gap energy for the studied structures. Both physical quantities reflect the reactivity of a given compound. TDM is increased as the chemical reactivity increased. Meanwhile, decreasing the HOMO/LUMO band gap energy is also a descriptor for increasing the reactivity of a given chemical structure [[36-37]. For P_4O_{10} structure, the TDM is 0.0000 Debye; the band gap was 12.3622 eV. For P_4O_{10} -ZnO-CaO structure, the TDM is increased to 6.1981 Debye, and the bandgap energy is decreased to 3.5391 eV. This indicated that both metal oxides are increasing the reactivity of P_4O_{10} structure. The effect of Li, Na, and K upon the reactivity of P_4O_{10} -ZnO-CaO is also indicated in the same table. The TDM for P_4O_{10} -ZnO-CaO-Li is increased to be 23.5878 Debye; the bandgap energy is further decreased to be 1.4947 eV. The same quantities for P_4O_{10} -ZnO-CaO-Na are respectively 27.9715 Debye and 1.1715 eV. Finally, the TDM and bandgap energy became 27.8134 Debye, 2.0588 eV corresponding to P_4O_{10} -ZnO-CaO-K. Regarding these results, one can conclude that metal oxides in nanoscale such as ZnO and CaO increase the reactivity of P_4O_{10} . Further reactivity of such a system is achieved as far as easily ignitable elements are introduced to such a system. The ability of a given surface to interact with its surrounding medium is measured with another important physical quantity, which is

the molecular electrostatic potential (MESP) that calculated at HF/3-21G** level and indicated in Figures 1-c and 2-c. More specifically, MESP is displayed by charge distribution revolving around the molecule space. It is considered as an important parameter for understanding both the electrophilic and nucleophilic attacks sites for biological recognition [38]; this is, of course, for biological interactions process. More generally, it could be an indication of hydrogen bonding interactions [39] in material science. So that, the MESP is predicting the reactive molecular sites for the studied structures. The MESP map and contour are indicated by colors whereas, different values of the electrostatic potential at the surface are represented by different colors. Potential is following the increasing orders: red < orange < yellow < green < blue. Where blue indicates the highest electrostatic potential energy, and red indicates the lowest electrostatic potential energy [[40]. Intermediary colors represent intermediary electrostatic potentials. They are introducing metal oxides as well as other metals, increasing the reactivity of the studied structure.

Table 1. Calculated HF/3-21G** total dipole moment and HOMO/LUMO band gap energy for the studied structures.

Structure	Total dipole moment Debye	HOMO/LUMO eV
P ₄ O ₁₀	0.0000	12.3622
P ₄ O ₁₀ -ZnO-CaO	6.1981	3.5391
P ₄ O ₁₀ -ZnO-CaO-Li	23.5878	1.4947
P ₄ O ₁₀ -ZnO-CaO-Na	27.9715	1.1715
P ₄ O ₁₀ -ZnO-CaO- K	27.8134	2.0588

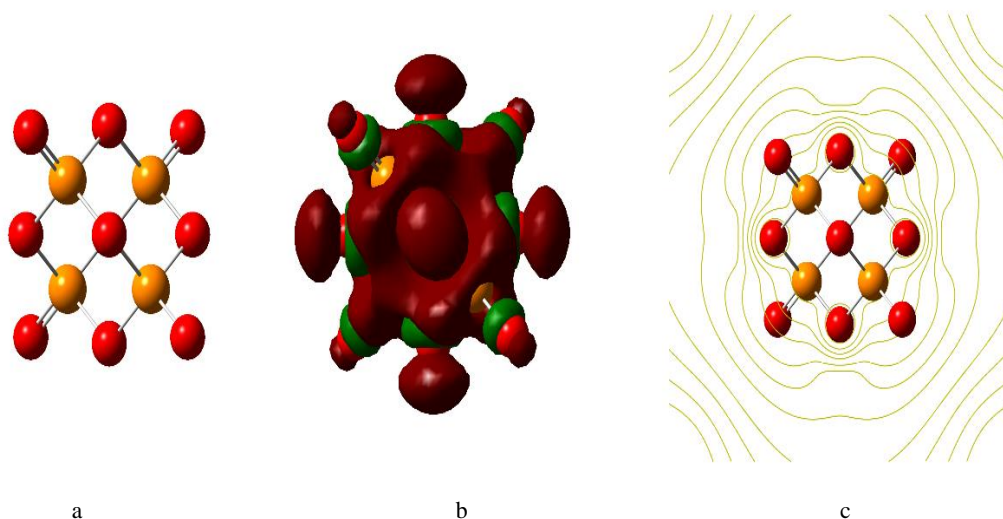


Figure 1. HF/3-21G** calculated structures for a- P₄O₁₀, b- HOMO/LUMO for P₄O₁₀ and c- MESP for P₄O₁₀.

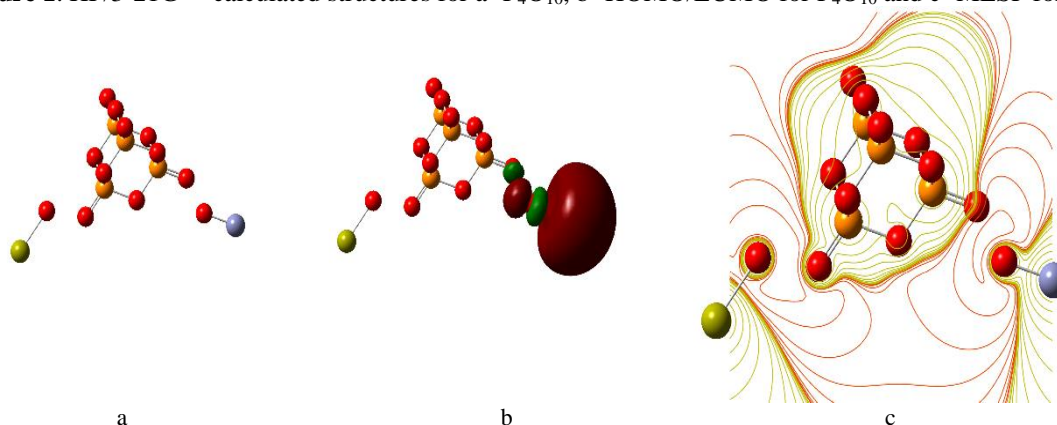


Figure 2. HF/3-21G** calculated structures for a- P₄O₁₀-ZnO-CaO, b- HOMO/LUMO for P₄O₁₀-ZnO-CaO and c- MESP for P₄O₁₀-ZnO-CaO.

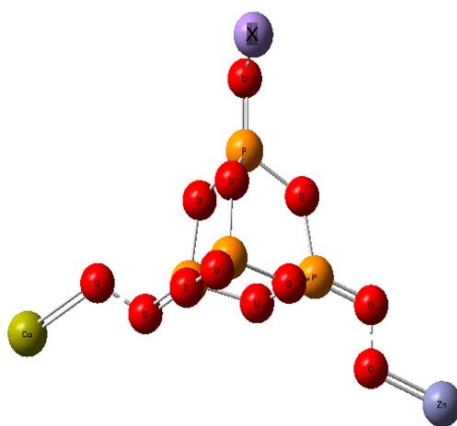


Figure 3. HF/3-21G** calculated structures for P_4O_{10} -ZnO-CaO-X; where X is Li; Na and K respectively.

4. Conclusions

Molecular modeling, a cost-effective, safe, and easy-to-use tool helps to investigate, interpret, explain, and identify molecularly. properties of many systems and structures. In this work, it is applied at HF level to study the effect of alkali on the electronic properties of Phosphate (P_4O_{10}) metal-oxide glass (ZnO&CaO). TDM, HOMO/LUMO bandgap, and MESP are reflecting the reactivity of the studied structures. TDM is increased by decreasing the HOMO/LUMO bandgap as a result of doping. This is an indication that the studied metal oxides in nanoscale increase the reactivity of P_4O_{10} glass. The calculated MESP indicted the active sites in the studied glass structure, which changes with changing the studied alkalis.

Funding

This research received no external funding.

Acknowledgments

The authors express their appreciation to "The Research Center for Advanced Materials Science (RCAMS)" at King Khalid University for funding this work under grant number RCAMS/KKU/016-20.

Conflicts of Interest

The authors declare no conflict of interest.

References

1. Brow, R.K. Review: the structure of simple phosphate glasses. *Journal of Non-Crystalline Solids* **2000**, *263-264*, 1-28, [https://doi.org/10.1016/S0022-3093\(99\)00620-1](https://doi.org/10.1016/S0022-3093(99)00620-1).
2. Brow, R.K.; Kovacic, L.; Loehman, R.E. Novel Glass Sealing Technologies. *Ceram. Trans.* **1996**, *177*, 70-88.
3. Day, D.E.; Wu, Z.; Ray, C.S.; Hrma, P. Chemically durable iron phosphate glass wastefoms. *Journal of Non-Crystalline Solids* **1998**, *241*, 1-12, [https://doi.org/10.1016/S0022-3093\(98\)00759-5](https://doi.org/10.1016/S0022-3093(98)00759-5)
4. Herms, G.; Sakowski, J.; Gerike, W.; Hoppe, U.; Stachel, D. Short-range and medium-range order in solid and molten metaphosphate glasses. *Journal of Non-Crystalline Solids* **1998**, *232-234*, 427-433, [https://doi.org/10.1016/S0022-3093\(98\)00472-4](https://doi.org/10.1016/S0022-3093(98)00472-4).
5. Karabulut, M.; Melnik, E.; Stefan, R.; Marasinghe, G.K.; Ray, C.S.; Kurkjian, C.R.; Day, D.E. Mechanical and structural properties of phosphate glasses. *Journal of Non-Crystalline Solids* **2001**, *288*, 8-17, [https://doi.org/10.1016/S0022-3093\(01\)00615-9](https://doi.org/10.1016/S0022-3093(01)00615-9).

6. Goj, P.; Stoch, P. Molecular dynamics simulations of $P_2O_5-Fe_2O_3-FeO-Na_2O$ glasses. *Journal of Non-Crystalline Solids* **2018**, *500*, 70-77, <https://doi.org/10.1016/j.jnoncrysol.2018.06.018>.
7. Sułowska, J.; Waclawska, I.; Szumera, M. Comparative study of zinc addition effect on thermal properties of silicate and phosphate glasses. *Journal of Thermal Analysis and Calorimetry* **2016**, *123*, 1091-1098, <https://doi.org/10.1007/s10973-015-5044-8>.
8. Qaysi, M.A.; Petrie, A.; Shah, R.; Knowles, J.C. Degradation of zinc containing phosphate-based glass as a material for orthopedic tissue engineering. *Journal of Materials Science: Materials in Medicine* **2016**, *27*, 157, <https://doi.org/10.1007/s10856-016-5770-x>.
9. Wan, M.H.; Wong, P.S.; Hussin, R.; Lintang, H.O.; Endud, S. Physical and Optical Properties of Calcium Zinc Borophosphate Glasses Doped with Manganese Ions. *Spectroscopy Letters* **2015**, *48*, 473-480, <https://doi.org/10.1080/00387010.2014.892512>.
10. Koudelka, L.; Jiráček, J.; Mošner, P.; Montagne, L.; Palavit, G. Study of lithium–zinc borophosphate glasses. *Journal of Materials Science* **2006**, *41*, 4636-4642, <https://doi.org/10.1007/s10853-006-0031-x>.
11. Youness, R.A.; Taha, M.A.; Elhaes, H.; Ibrahim, M. Molecular modeling, FTIR spectral characterization and mechanical properties of carbonated-hydroxyapatite prepared by mechanochemical synthesis. *Materials Chemistry and Physics* **2017**, *190*, 209-218, <https://doi.org/10.1016/j.matchemphys.2017.01.004>.
12. Galal, A.M.F.; Atta, D.; Abouelsayed, A.; Ibrahim, M.A.; Hanna, A.G. Configuration and molecular structure of 5-chloro-N-(4-sulfamoylbenzyl) salicylamide derivatives. *Spectrochim Acta A* **2019**, *214*, 476-486, <https://doi.org/10.1016/j.saa.2019.02.070>.
13. Abdelsalam, H.; Teleb, N.H.; Yahia, I.S.; Zahran, H.Y.; Elhaes, H.; Ibrahim, M.A. First principles study of the adsorption of hydrated heavy metals on graphene quantum dots. *Journal of Physics and Chemistry of Solids* **2019**, *130*, 32-40, <https://doi.org/10.1016/j.jpjcs.2019.02.014>.
14. Abdelsalam, H.; Saroka, V.A.; Ali, M.; Teleb, N.H.; Elhaes, H.; Ibrahim, M.A. Stability and electronic properties of edge functionalized silicene quantum dots: A first principles study. *Physica E: Low-dimensional Systems and Nanostructures* **2019**, *108*, 339-346, <https://doi.org/10.1016/j.physe.2018.07.022>.
15. Mahmoud, A.A.; Osman, O.; Elhaes, H.; Ferretti, M.; Fakhry, A.; Ibrahim, M.A. Computational Analyses for the Interaction Between Aspartic Acid and Iron. *Journal of Computational and Theoretical Nanoscience* **2018**, *15*, 470-473, <https://doi.org/10.1166/jctn.2018.7113>.
16. Abdel-Gawad, F.K.; Osman, O.; Bassem, S.M.; Nassar, H.F.; Temraz, T.A.; Elhaes, H.; Ibrahim, M. Spectroscopic analyses and genotoxicity of dioxins in the aquatic environment of Alexandria. *Marine Pollution Bulletin* **2018**, *127*, 618-625, <https://doi.org/10.1016/j.marpolbul.2017.12.056>.
17. Elhaes, H.; Attallah, M.; Elbasha, Y.; Al-Alousi, A.; El-Okr, M.; Ibrahim, M. Modeling and Optical Properties of $P_2O_5-ZnO-CaO-Na_2O$ Glasses Doped with Copper Oxide. *Journal of Computational and Theoretical Nanoscience* **2014**, *11*, 2079-2084, <https://doi.org/10.1166/jctn.2014.3608>.
18. Hermansen, C.; Mauro, J.C.; Yue, Y. A model for phosphate glass topology considering the modifying ion sub-network. *The Journal of Chemical Physics* **2014**, *140*, <https://doi.org/10.1063/1.4870764>.
19. Christie, J.K.; Ainsworth, R.I.; Di Tommaso, D.; de Leeuw, N.H. Nanoscale Chains Control the Solubility of Phosphate Glasses for Biomedical Applications. *The Journal of Physical Chemistry B* **2013**, *117*, 10652-10657, <https://doi.org/10.1021/jp4058115>.
20. Christie, J.K.; Ainsworth, R.I.; Hernandez, S.E.R.; de Leeuw, N.H. Structures and properties of phosphate-based bioactive glasses from computer simulation: a review. *Journal of Materials Chemistry B* **2017**, *5*, 5297-5306, <https://doi.org/10.1039/C7TB01236E>.
21. Ainsworth, R.I.; Tommaso, D.D.; Christie, J.K.; de Leeuw, N.H. Polarizable force field development and molecular dynamics study of phosphate-based glasses. *The Journal of Chemical Physics* **2012**, *137*, <https://doi.org/10.1063/1.4770295>.
22. Di Tommaso, D.; Ainsworth, R.I.; Tang, E.; de Leeuw, N.H. Modelling the structural evolution of ternary phosphate glasses from melts to solid amorphous materials. *Journal of Materials Chemistry B* **2013**, *1*, 5054-5066, <https://doi.org/10.1039/C3TB20662A>.
23. Wang, J.; Li, B.; Zhang, X.; Hu, Q.; Yu, W.; Wang, H.; Duan, D.; Li, J.; Zhao, B. Docking and molecular dynamics studies on the mechanism of phospholipase D-mediated transphosphatidylolation to construct the reaction kinetic model: Application in phosphatidylserine production. *Journal of the Taiwan Institute of Chemical Engineers* **2019**, *96*, 82-92, <https://doi.org/10.1016/j.jtice.2018.12.012>.
24. Liu, B.; Zhou, K. Recent progress on graphene-analogous 2D nanomaterials: Properties, modeling and applications. *Progress in Materials Science* **2019**, *100*, 99-169, <https://doi.org/10.1016/j.pmatsci.2018.09.004>.
25. Saleh, N.; Mostafa, A.A.; Omar, A.; Elhaes, H.; Ibrahim, M. Molecular Modeling Analyses of Modified Polyvinylalcohol/Hydroxyapatite Composite. *Journal of Computational and Theoretical Nanoscience* **2017**, *14*, 2298-2301, <https://doi.org/10.1166/jctn.2017.6823>.
26. Ibrahim, A.; Elhaes, H.; Ibrahim, M.; Computational Notes on the Electronic Properties of Carboxylic Acid, *Letters in Applied NanoBioScience*. **2020**, *9* (2), 1079-1082. <https://doi.org/10.33263/LIANBS92.10791082>
27. Ahmed, R.; Hanan, E.; Nabila, S.A.; Hanan, S.I.; Medhat, I. Green Route for the Removal of Pb from Aquatic Environment. *Combinatorial Chemistry & High Throughput Screening* **2020**, *23*, 1-12, <https://doi.org/10.2174/1386207323666200127123349>.

28. Bayoumy, A.M.; Refaat, A.; Yahia, I.S.; Zahran, H.Y.; Elhaes, H.; Ibrahim, M.A.; Shkir, M. Functionalization of graphene quantum dots (GQDs) with chitosan biopolymer for biophysical applications. *Optical and Quantum Electronics* **2019**, *52*, 5986-5993. <https://doi.org/10.1007/s11082-019-2134-z>.
29. Macias-Jamaica, R.E.; Castrejón-González, E.O.; González-Alatorre, G.; Alvarado, J.F.J.; Díaz-Ovalle, C.O. Molecular models for Sodium Dodecyl Sulphate in aqueous solution to reduce the micelle time formation in molecular simulation. *Journal of Molecular Liquids* **2019**, *274*, 90-97, <https://doi.org/10.1016/j.molliq.2018.10.121>.
30. Abdel-Karim, A. Elhaes, H.; El-Kalliny, A. S.; Badawy, M. I.; Ibrahim, M.; Gad-Allah, T.G. Probing Protein rejection behavior of blended PES-based flat-sheet ultrafiltration membranes: A density functional theory (DFT) study, *Spectrochimica Acta A* **2020**, 238. 118399. <https://doi.org/10.1016/j.saa.2020.118399>
31. Badry, R.; El-Khodary, S.; Elhaes, H.; Nada, N.; Ibrahim, M. On the molecular modeling analyses of sodium carboxymethyl cellulose treated with acetic acid. *Letters in Applied NanoBioScience* **2019**, *8*, 553-557, <https://doi.org/10.33263/LIANBS.82.553557> .
32. El-Mansy, M. A. M.; Osman, O.; Mahmoud, A-A.; Elhaes, H.; Ibrahim, M.; Computational Notes on the Molecular Modeling Analyses of Flutamide, *Letters in Applied NanoBioScience* **2020**, *9* (2), 1099-1102. <https://doi.org/10.33263/LIANBS92.10991102>
33. Selim, A.Q.; Sellaoui, L.; Mobarak, M. Statistical physics modeling of phosphate adsorption onto chemically modified carbonaceous clay. *Journal of Molecular Liquids* **2019**, *279*, 94-107, <https://doi.org/10.1016/j.molliq.2019.01.100>.
34. Donnini, J.; Chiappini, G.; Lancioni, G.; Corinaldesi, V. Tensile behaviour of glass FRCM systems with fabrics' overlap: Experimental results and numerical modeling. *Composite Structures* **2019**, *212*, 398-411, <https://doi.org/10.1016/j.compstruct.2019.01.053>.
35. Gaussian 09, Revision C.01, M. J. Frisch, G. W. Trucks, H. B. Schlegel, G. E. Scuseria, M. A. Robb, J. R. Cheeseman, G. Scalmani, V. Barone, B. Mennucci, G. A. Petersson, H. Nakatsuji, M. Caricato, X. Li, H. P. Hratchian, A. F. Izmaylov, J. Bloino, G. Zheng, J. L. Sonnenberg, M. Hada, M. Ehara, K. Toyota, R. Fukuda, J. Hasegawa, M. Ishida, T. Nakajima, Y. Honda, O. Kitao, H. Nakai, T. Vreven, J. A. Montgomery, Jr., J. E. Peralta, F. Ogliaro, M. Bearpark, J. J. Heyd, E. Brothers, K. N. Kudin, V. N. Staroverov, T. Keith, R. Kobayashi, J. Normand, K. aghavachari, A. Rendell, J. C. Burant, S. S. Iyengar, J. Tomasi, M. Cossi, N. Rega, J. M. Millam, M. Klene, J. E. Knox, J. B. Cross, V. Bakken, C. Adamo, J. Jaramillo, R. Gomperts, R. E. Stratmann, O. Yazyev, A. J. Austin, R. Cammi, C. Pomelli, J. W. Ochterski, R. L. Martin, K. Morokuma, V. G. Zakrzewski, G. A. Voth, P. Salvador, J. J. Dannenberg, S. Dapprich, A. D. Daniels, O. Farkas, J. B. Foresman, J. V. Ortiz, J. Cioslowski, and D. J. Fox, Gaussian, Inc., Wallingford CT **2010**.
36. Ibrahim, M.; Elhaes, H. Computational Spectroscopic Study of Copper, Cadmium, Lead and Zinc Interactions in the Environment. *Int. J. Environment and Pollution* **2005**, *23*, 417-424, <https://doi.org/10.1504/IJEP.2005.007604>.
37. Ibrahim, M.; Mahmoud, A.A. Computational Notes on the Reactivity of Some Functional Groups. *Journal of Computational and Theoretical Nanoscience* **2009**, *6*, 1523-1526, <https://doi.org/10.1166/jctn.2009.1205>.
38. Politzer, P.; Laurence, P.R.; Jayasuriya, K. Molecular electrostatic potentials: an effective tool for the elucidation of biochemical phenomena. *Environ Health Perspect* **1985**, *61*, 191-202, <https://doi.org/10.1289/ehp.8561191>.
39. Politzer, P.; Murray, J.S. Relationships of Electrostatic Potentials to Intrinsic Molecular Properties, *J.Theor.Comput.Chem.* **1996**, *3*, 649-660, [https://doi.org/10.1016/S1380-7323\(96\)80056-2](https://doi.org/10.1016/S1380-7323(96)80056-2).
40. Şahin, Z.S.; Şenöz, H.; Tezcan, H.; Büyükgüngör, O. Synthesis, spectral analysis, structural elucidation and quantum chemical studies of (E)-methyl-4-[(2-phenylhydrazono)methyl]benzoate. *Spectrochimica Acta Part A* **2015**, *143*, 91-100, <https://doi.org/10.1016/j.saa.2015.02.032>.